Supporting Information for

Unusual Pressure Response of Vibrational Modes in Anisotropic TaS$_3$

Kedi Wu,[†] Bin Chen,[†] Hui Cai,[†] Mark Blei,[†] Juliana Bennett,[†] Shengxue Yang,[‡] David Wright,[§] Yuxia Shen,[†] and Sefaattin Tongay[*,†]

[†] School for Engineering of Matter, Transport and Energy, Arizona State University, Tempe, Arizona 85287, United States

[‡] School of Materials Science and Engineering, Beihang University, Beijing 100191, People's Republic of China

[§] LeRoy Eyring Center for Solid State Science, Arizona State University, Tempe, Arizona 85287, United States

Corresponding Author: Sefaattin Tongay
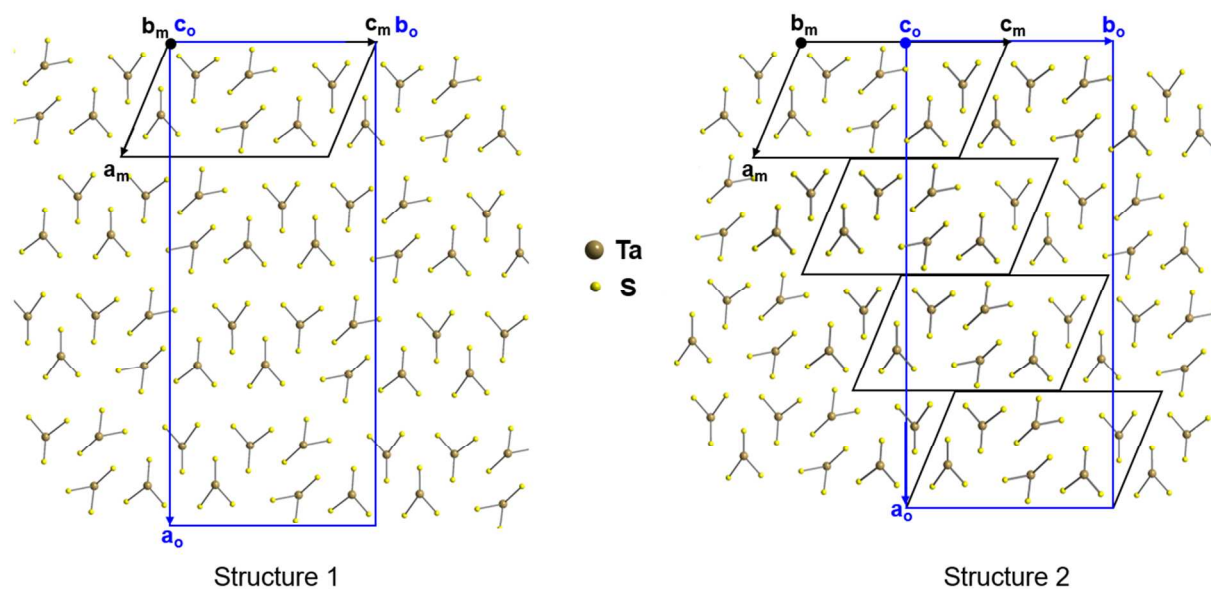
E-mail: sefaattin.tongay@asu.edu

Figure S1 Two potential unit cell structures of orthorhombic-TaS$_3$ (*o*-TaS$_3$).
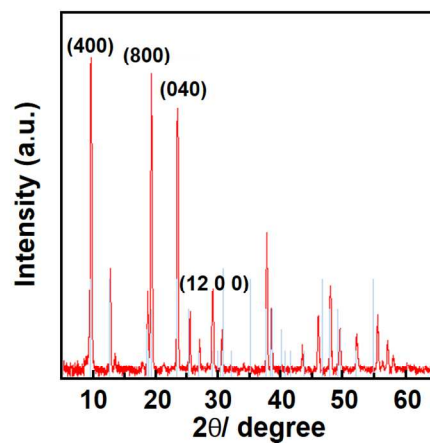
Figure S2 X-ray diffraction (XRD) pattern of *o*-TaS$_3$.

Figure S3 Schematic diagram for S$_\parallel$, S$_\perp$, A$_g$ and A$_g^{s\text{-}s}$ modes.

Figure S4 Angle-resolved Raman spectroscopy (polar plots) for additional the Raman peaks of *o*-TaS$_3$ under excitation wavelength of $\lambda = 532$ nm.
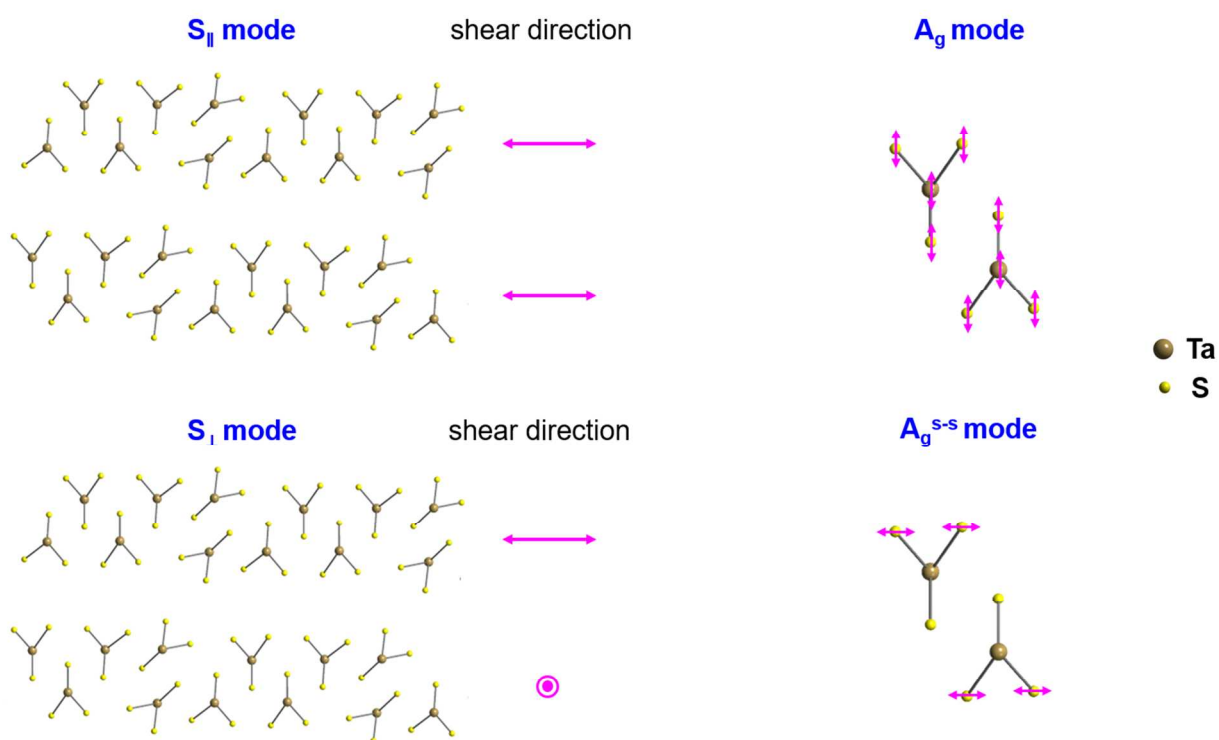
Figure S5 Comparison between the angle-resolved Raman response (polar plots) of *o*-TaS$_3$ under three different excitation wavelengths: $\lambda = 488$ nm, 532 nm, 633 nm.
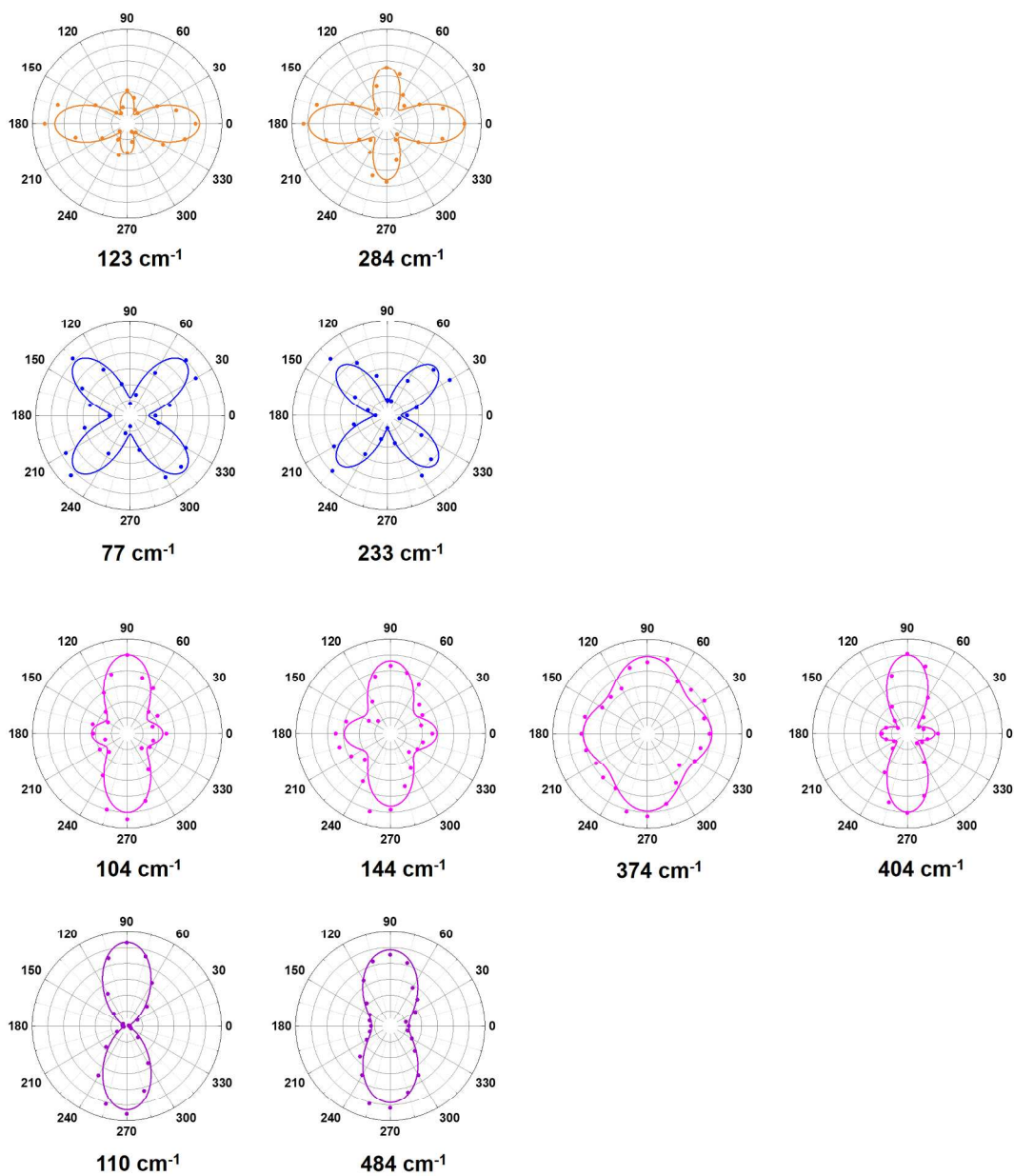

Structure 1   Structure 2

Figure S1 Two potential unit cell structures of orthorhombic-TaS$_3$ (blue line) described as stacking four slabs of *m*-TaS$_3$ unit cells (black line).
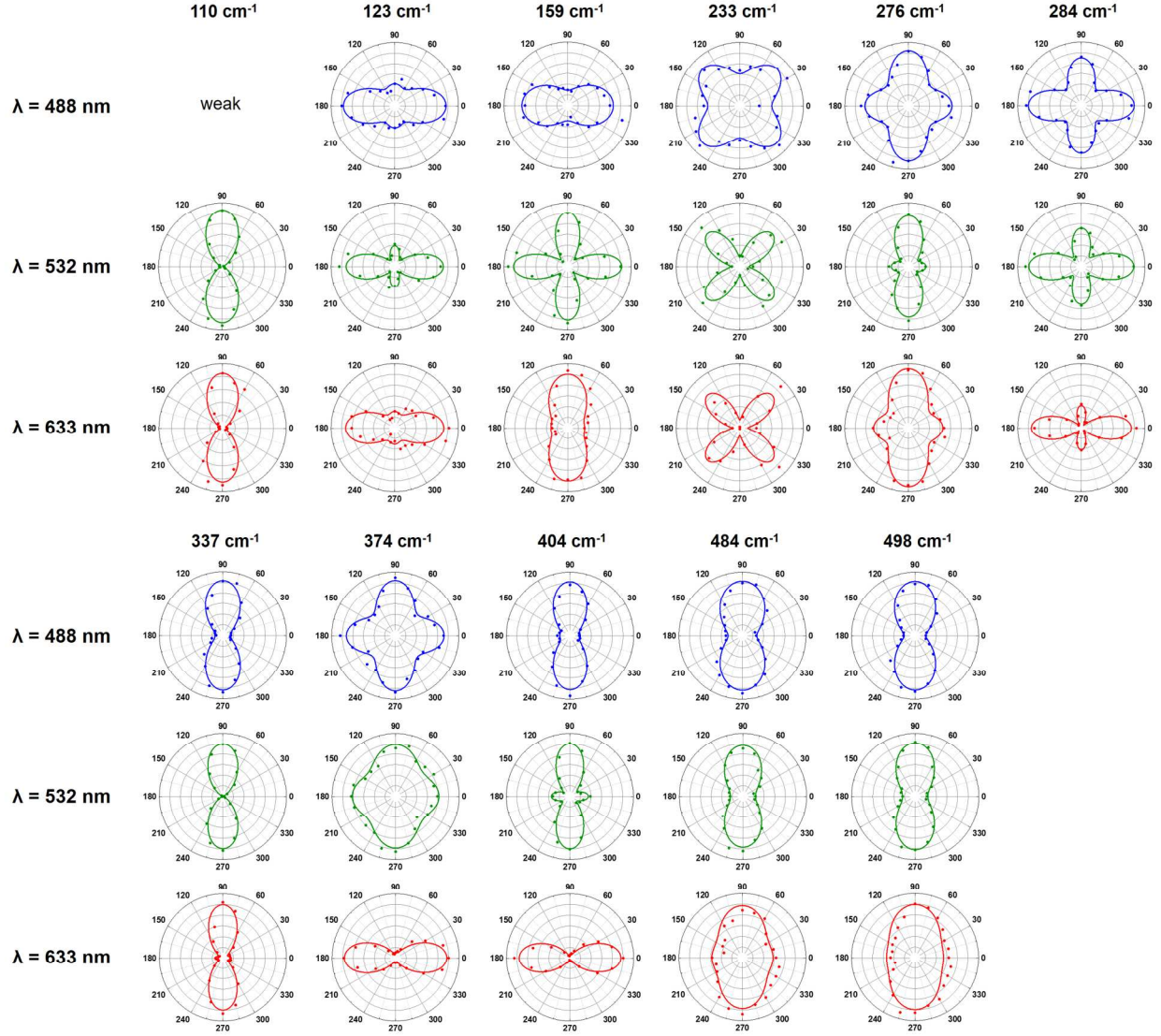
Figure S2 X-ray diffraction (XRD) pattern of o-TaS$_3$.

Figure S3 Schematic diagram for S$_∥$, S$_⊥$, A$_g$ and A$_g^{s-s}$ modes.

Figure S4 Angle-resolved Raman spectroscopy (polar plots) for additional the Raman peaks of o-TaS$_3$ under excitation wavelength of $\lambda = 532$ nm.

Figure S5 Comparison between the angle-resolved Raman response (polar plots) of o-TaS₃ under three different excitation wavelengths: λ = 488 nm, 532 nm, 633 nm, respectively.